Forest and Society
Vol. 8(2): 314-330, December 2024
doi: 10.24259/fs.v8i2.32194

REGULAR RESEARCH ARTICLE

Spatial Patterns of Cumulative Hotspots and Their Relationships with Topographical Factors and Land Use in Kanchanaburi Province, Thailand

Pornperm Sae-ngow [1], Chudech Losiri [1, *], and Asamaporn Sitthi [1]

AFFILIATIONS

[1.] Department of Geography, Faculty of Social Sciences, Srinakharinwirot University, Bangkok, Thailand.
*Corresponding author: chudech@g.swu.ac.th

RECEIVED 2023-12-08
ACCEPTED 2024-03-27

ABSTRACT

The clustering of hotspots represents fires occurring at specific locations across various time intervals, and is an increasingly important interdisciplinary research phenomenon. This article investigates the spatial distribution of cumulative hotspots and their relationships with topographical factors and land use in Kanchanaburi province. Data from the Suomi NPP VIIRS system spanning from 2012 to 2021 were utilized for the analysis of Getis-Ord (Gi*) spatial autocorrelation using Fire Radiative Power values. The analysis included the correlation with topographic data such as elevation, slope, aspect, and overlay with land use data. The results reveal that significant hotspots are concentrated in the districts of Si Sawat, Thong Pha Phum, Sai Yok, Sangkhla Buri, and Mueang Kanchanaburi. The majority of hotspots were statistically insignificant (85%), with hotspots (10%) and cold spots (5%) predominantly occurring in forested and agricultural areas. Hotspots were particularly prevalent in the northern and northeastern regions. Therefore, the utilization of Suomi NPP VIIRS data in conjunction with spatial statistics can identify the occurrence of hotspots and cold spots, aiding in planning and policy-making efforts to mitigate hotspot occurrences.

KEYWORDS

Spatial pattern; Fire; Hotspots; Land use; Spatial statistics; Thailand.

1. INTRODUCTION

Wildfires and hotspot occurrences have gained significant attention from numerous countries and research fields. The analysis of Atmospheric Infrared Sounder (AIRS) radiation data from NASA's Aqua satellite and the active fire product derived from VIIRS instruments onboard the Suomi National Polar-orbiting Partnership (S-NPP) and NOAA-20 satellites indicates an increasing rate of forest fire occurrences, contributing to elevated stress on environmental systems and global atmospheric conditions (Tzoumas et al., 2023; Vadrevu et al., 2022; Yu et al., 2024). For the Thailand context, we have gathered Standard Processing of active fire data from the Moderate Resolution Imaging Spectroradiometer (MODIS) on the Aqua and Terra satellites, sourced through the Fire Information for Resource Management Systems. Subsequently, we conducted data management and presented it as the annual cumulative quantity of hotspots. The findings indicate that the cumulative hotspot quantity exhibited fluctuations during the period from 2011 to 2020. In 2011, there were 19,326 cumulative hotspots, gradually increasing to 30,029 in 2016, followed by a decline to 18,563 and 18,089 hotspots in 2017 and 2018, respectively. The years 2020 and 2021 saw a gradual increase to 30,233 hotspots. The annual average hotspot quantity was determined to be 27,223 (FIRMS, 2020). Consequently, the increasing accumulation of annual hotspot quantities poses a significant issue, underlying the open burning problem that contributes to the generation of air pollutants, and has repercussions for everyone. This issue is closely tied to both life and property, prompting the Thailand Department of Pollution Control to establish a national master plan on open burning control. This encompasses the burning of agricultural residues, community waste incineration, and forest fires

(Department of Pollution Control, 2020).

Kanchanaburi is a province of great importance in terms of natural resources, as it is the source of numerous rivers and includes national parks such as Khao Laem National Park, Srinakarin Dam National Park, Chaloem Rattanakosin National Park, Sai Yok National Park, Lam Khlong Ngu National Park, Thong Pha Phum National Park, Erawan National Park, and several water reservoirs, including Mae Klong Dam, Vajiralongkorn Dam, and Srinakarin Dam. Based on MODIS satellite data from FIRMS, the cumulative quantity of hotspots in the province was 650 in the year 2011 and steadily increased to 1,908 hotspots in the year 2020 (FIRMS, 2020). This illustrates the continuous rise in cumulative hotspot occurrences in the province of Kanchanaburi over the past decade. From the wildfire report for the year 2020 by the Geo-Informatics and Space Technology Development Agency of Thailand, it was observed that Kanchanaburi Province had a cumulative quantity of hotspots detected by the SUOMI NPP VIIRS satellite system, totaling 14,637 hotspots. The majority of these hotspots occurred in forested areas, accounting for 87.5% of the total hotspots in the province. Agricultural areas, community zones, and urban areas collectively represented 12.2% of the total hotspot occurrences in Kanchanaburi (Geo-Informatics and Space Technology Development Agency (Public Organization), 2020). This has resulted in increased temperatures and environmental pollution, impacting lives, health, and property (Kumharn et al., 2023; Wongnakae et al., 2023). Furthermore, the occurrence of wildfires and hotspots correlates with the incidence of forested areas, agricultural regions, and community zones, demonstrating a connection with human activities. For example, forest burning to promote grass regrowth for livestock grazing and burning in agricultural fields for soil preparation before planting are illustrative instances of such human activities (Phonphan, 2020; Ye et al., 2017; Geo-Informatics and Space Technology Development Agency, 2020). Therefore, the incidences of fire, along with land use, presents a pertinent intersection of issues for research.

Numerous researchers have delved into the study of wildfires and hotspots using MODIS data (de México, 2017; Reddy et al., 2020), VIIRS data (Li et al., 2022; Vadrevu et al., 2019), and even compared the two datasets (Unnikrishnan & Reddy, 2020). The outcomes of these studies reveal that VIIRS is more detailed in detecting hotspots than MODIS, attributed to the finer resolution of VIIRS Thermal Band wavelength range compared to that of MODIS (Schroeder et al., 2014). MODIS has a sensor resolution of about 1,000 meters, while VIIRS has a resolution of about 375 meters. This makes it suitable for monitoring areas at risk of smaller hotspots, such as communities, cultivated areas, and agricultural areas less than 1 square kilometer in size (Fu et al., 2021; Li et al., 2022; Zhang et al., 2020). Additionally, the application of spatial statistics, such as the Getis-Ord Gi* hotspot analysis helps identify significant spatial clusters or patterns in the distribution of values, while Kernel Density provides a smoother representation of the spatial intensity or density of point features, has provided insight into hotspot occurrences, their overall patterns and relationships with various environmental factors, including topography, fire-prone fuels, land use and human activity factor (Cizungu et al., 2021; Mupfiga et al., 2022; Zúñiga-Vásquez & Pompa-García, 2019).

This research article aims to achieve three main objectives: 1) Study the spatial pattern of cumulative hotspots, involving the analysis of annual changes in hotspot occurrence spanning from 2012 to 2021, 2) Examine the relationship between topographical factors and the spatial pattern of cumulative hotspots, and 3) Investigate the relationship between land use and spatial pattern of cumulative hotspots. To achieve these objectives, this study employs spatial statistics in conjunction with VIIRS

data from the Suomi National Polar-orbiting Partnership (Suomi NPP) and land use information specific to Kanchanaburi Province. The outcomes are intended to assist managers of the protected area in implementing specific measures for fire management both before and after fire incidents. Additionally, the findings aim to contribute to the development of policies and strategies that address environmental concerns arising from hotspot occurrences.

2. MATERIALS AND METHODS

2.1 Study area

Kanchanaburi Province is located in the western region of Thailand and shares its borders with Myanmar. It is the third-largest province in the country, characterized by an expansive landscape dominated by forests and mountains, which can be categorized into the following three geographical zones: 1) Mountainous and Highland Zone: This zone is situated in the northern part of the province and includes areas within Sangkhla Buri, Thong Pha Phum, Si Sawat, and Sai Yok districts. 2) Plateau and Hilly Zone: Located in the northeastern part of the province, this zone features a mix of plateaus and hills. It covers areas within Lao Khwan, Bo Phloi, and Phanom Thuan districts. 3) River Basin Zone: Located in the southern part of the province, this zone comprises fertile plains with productive soil. It encompasses areas within Tha Maka, Tha Muang, and Mueang Kanchanaburi districts. The total land area of the province is approximately 19,473 square kilometers. Agricultural land accounts for 4,250 square kilometers (22% of the total land area). The distribution of agricultural land use is as follows: rice fields cover 674 square kilometers (3%), field crops occupy 2523 square kilometers (13%), orchards and perennial crops span 494 square kilometers (3%), flower and decorative plants encompass 287 square kilometers (1%), and other agricultural uses utilize 271 square kilometers (1%). Non-agricultural land comprises 3,140 square kilometers (16%), while the remaining 11,995 square kilometers constitutes forest area (62%) (Kanchanaburi Provincial Statistics Report 2022). These study area details are depicted in Figure 1.

2.2 Data used and source

Figure 2 describes the research framework for data collection, data preparation, and data analysis. The study begins with the data collection process including gathering of information land use, topographic data, administrative boundaries, and cumulative hotspots detected by the Suomi NPP satellite's VIIRS system from 2012 to 2021, obtained from NASA's Fire Information for Resource Management System (FIRMS), as shown in Table 1.

2.2.1 Suomi National Polar-orbiting Partnership (S-NPP)

Visible Infrared Imaging Radiometer Suite (VIIRS) is a sensor suite part of the Joint Polar Satellite System (JPSS), a program led by the National Aeronautics and Space Administration (NASA) and the National Oceanic and Atmospheric Administration (NOAA). Designed with the objective of systematically acquiring data concerning diverse facets of the Earth's atmosphere, oceans, and terrestrial surfaces, VIIRS operates as a component of polar-orbiting satellites within the JPSS, such as the Suomi National Polar-orbiting Partnership (NPP) satellite. Its capacity extends to capturing imagery across multiple spectral bands, including those in visible, infrared, and thermal wavelengths (Schroeder et al., 2014). In this study we utilize satellite fire hotspot products in Kanchanaburi Province for the period 2012–2022 from NASA's Fire Information for Resource Management System (FIRMS).

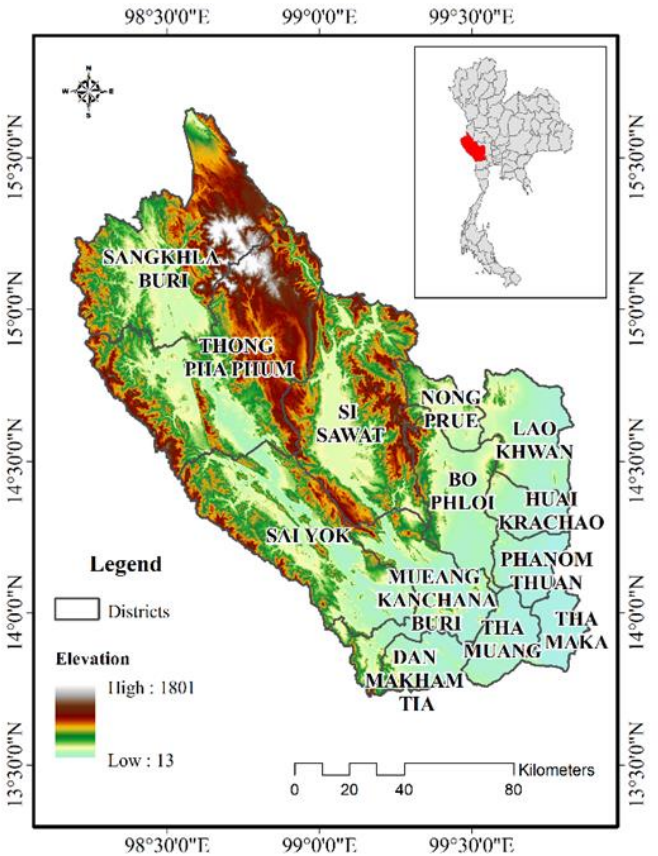

Figure 1. Study area - Kanchanaburi Province

2.2.2 Terrain

NASADEM, a reprocessing of SRTM data with improved accuracy through the integration of auxiliary information from ASTER GDEM, ICESat GLAS, and PRISM datasets, is distributed in 1-degree latitude by 1-degree longitude tiles. It covers all land between 60° N and 56° S latitude, encompassing approximately 80% of Earth's total landmass (NASA JPL, 2020).

Table 1. Data Used in the Research

Dataset	Resolution/scale	Source
Suomi National Polar-orbiting Partnership (S-NPP) satellite: VIIRS Systems (2012-2021)	375 meters	FIRMS (accessed on 20 January 2023)
Terrain	30 meters	NASA JPL (accessed on 20 April 2023
Land Use	Scale: 1: 25,000	Land Development Department (accessed on 20 January 2023)
Administrative boundaries	Scale: 1: 25,000	Department Of Provincial Royal Thai Survey Department (accessed on 20 January 2023)

2.2.3 Land use

Land-use data were sourced from the Department of Land Development in Thailand. The map scale employed for overlay analysis was 1:25,000, and the land-use data were classified into five categories: U (Urban and Built-up Land), A (Agricultural Land), F (Forest Land), W (Water Resource), and M (Miscellaneous). The dataset can be accessed from the official website: http://webapp.ldd.go.th/Soilservice/ (Land Development Department, 2023).

2.2.4 Administrative boundaries

Administrative boundaries for Thailand at levels 0 (country), 1 (province), 2 (district), and 3 (sub-district) were obtained from the Royal Thai Survey Department and can be downloaded from the following link: https://data.humdata.org/dataset/cod-ab-tha (Royal Thai Survey Department, 2023).

2.3 Methodology

To identify the spatial pattern of fire spots and the association between fire intensity and relevant factors, this study elaborates applies an overall methodology as shown in Figure 2, detailed by the following steps.

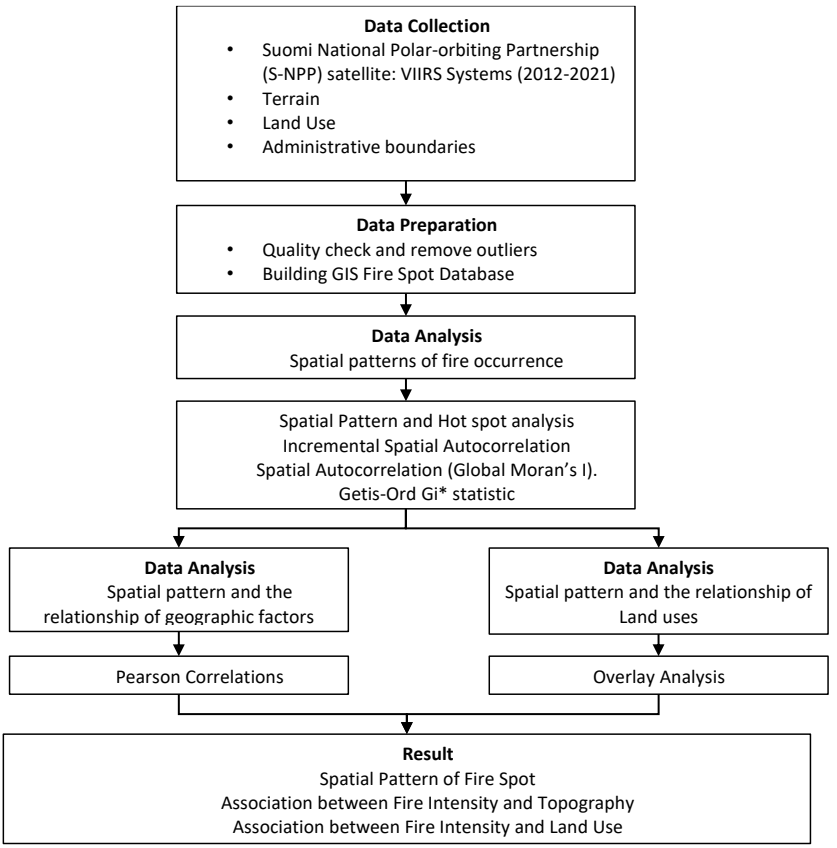

Figure 2. Research Framework and Concept

2.3.1 Data preparation for analysis

The data preparation process starts by managing the cumulative hotspot data from the Suomi NPP satellite's VIIRS system for the years 2012 to 2021. The data was transformed into spatial data sets from Kanchanaburi Province's original comma-separated values text file format, totaling 81,464 locations. Low-confidence level data during daytime, reflecting high sunlight conditions, and abnormal low-temperature values (<15k) for the mid-infrared channel I4, are eliminated. Only the normal confidence level data which does not reflect high sunlight during daytime and abnormal strong temperature values (>15k) during both daytime and nighttime are retained. This process yields 70,868 remaining positions, which are verified for accuracy and used to establish a cumulative hotspot database for the subsequent cumulative hotspots spatial analysis concerning Kanchanaburi land use.

2.3.2 Analysis of annual cumulative hotspot changes from 2012 to 2021

Fire Radiative Power depicts the pixel-integrated fire radiative power in megawatts (FIRMS, 2020). This analysis utilizes fire radiative power data from the Suomi NPP satellite's VIIRS system to determine the spatial pattern during the period 2012-2021. The study investigates annual cumulative hotspot changes from 2012 to 2021, analyzing occurrence frequency annually and monthly (January to December). Additionally, it assesses monthly Fire Radiative Power (FRP) using data from the Suomi NPP satellite's VIIRS system. FRP is classified into four categories: 'VERY LOW: VL' (≤ 15 MW), 'LOW: L' (15-40 MW), 'MODERATE: M' (40-80 MW), and 'HIGH: H' (> 80 MW) (Cizungu et al., 2021). This approach offers insights into hotspot intensities and spatial distribution.

2.3.3 Analysis of cumulative hotspots (hot spot analysis - getis-ord gi)*

The analysis commences with an overview of the spatial pattern of cumulative hotspots using the Global Moran's I index by Equation (1).

$$I = \frac{n}{w} * \frac{\sum\sum w_{ij}(x_i-\bar{x})(x_j-\bar{x})}{\sum(x_i-\bar{x})^2} \quad (1)$$

Where: I represents Moran's I Index, x_i and x_j denote the observed values of areas i and j respectively, $\bar{x}$ is the average of observed values, n is the number of observations, w is the sum of the spatial weight matrix, and w_{ij} represents the elements of the spatial weight matrix.

Spatial autocorrelation, as quantified by Global Moran's I, spanned a spectrum from -1 to +1. When falling within the interval of 0 to +1, these values pointed to a positive spatial relationship, indicative of a coherent spatial pattern. Conversely, values within the -1 to 0 range signified a negative spatial relationship, implying a fragmented spatial pattern. Lastly, when Global Moran's I registered a value of 0, it implied a random spatial distribution (Getis & Ord, 1992). The Incremental Spatial Autocorrelation analysis method is applied to determine an appropriate bandwidth, which is then used to create weighted values for analyzing hot and cold spots. The spatially weighted values is used for the spatial analysis of cumulative hotspot during 2012-2021 utilizing the Getis-Ord Gi* Hot Spot Analysis method.

The annual cumulative hotspots analysis (Getis-Ord Gi*) is a method used to examine the local Indicator of Spatial Association (LISA) statistics, aiming to explain the degree of clustering of the studied phenomenon in relation to neighboring areas through inferential statistics that will undergo hypothesis testing (Anselin, 1995). If the null hypothesis is accepted, it implies the absence of spatial clustering (Akyürek, 2023).

The findings are displayed through z-scores and p-values. Through an examination of the data at the focal point of interest, alongside data from neighboring points, the identification of hotspots (cluster locations of high-fire radiative power) and cold spots (cluster locations of low-fire radiative power) occurs. A high positive z-score for both the focal location and its surroundings signifies a Hotspot, whereas low negative z-scores for both locations indicate a cold spot.

The z-score holds statistical significance when the difference between the observed sum and the estimated sum of the focal and neighboring points significantly exceeds what would be considered a random pattern. It indicates that the null hypothesis can be rejected which implies the existence of spatial clustering (Getis & Ord, 1992; Hazaymeh et al., 2022; Lanorte et al., 2013; Mesquitela et al., 2022; Mpakairi et al., 2019).

$$G_i^* = \frac{\sum_{j=1}^{n} w_{i,j}x_j - \bar{X}\sum_{j=1}^{n} w_{i,j}}{s\sqrt{\frac{\left[n\sum_{j=1}^{n} w_{i,j}^2 - \left(\sum_{j=1}^{n} w_{i,j}\right)^2\right]}{n-1}}} \quad (2)$$

In spatial analysis, the Getis-Ord statistic (G_{i*}) is calculated using variables such as observed values (x_j), the average ($\bar{x}$), weights between locations (w_{ij}), standard deviation (s), and the total number of areas (n). G_{i*} values are indicative of spatial clustering or dispersion. Validation involves assessing the z-score and p-value for reliability in identifying significant spatial patterns.

2.3.4 Analyzing the relationship of geographic factors with spatial patterns of hotspot accumulation

The results of the spatial analysis of hotspot accumulation, using Hot Spot Analysis (Getis-Ord Gi*), were further examined to assess the relationship between the energy distribution characteristics of hotspots and cold spots with geographic factors. These factors include elevation, slope, and aspect. In order to explain the relationship between geographic factors and the occurrence of hotspots and cold spots, the Pearson correlation coefficient which is represented by the following Equation (3) was employed (Benesty, et al., 2009).

$$r_{xy} = \frac{N\sum XY - (\sum X)(\sum Y)}{\sqrt{[N\sum X^2 - (\sum X)^2][N\sum Y^2 - (\sum Y)^2}} \quad (3)$$

In evaluating the correlation between geographic factors (X) and Fire Radiative Power (Y), the coefficient of reliability (r_{xy}) is essential. It quantifies the strength and direction of the relationship and is derived from the correlation analysis. N represents the total number of data points considered in the analysis.

2.3.5 Analysis of the relationship between land use and spatial patterns of cumulative hotspots

The results of the spatial analysis of cumulative hotspots (Hot Spot Analysis (Getis-Ord Gi*)) were further analyzed by overlaying them with land-use data from the Department of Land Development in Thailand. The map scale used for the overlay was 1:25,000, and the land-use data was categorized into five types: U: Urban and Built-up Land, A: Agricultural Land, F: Forest Land, W: Water resource, and M: Miscellaneous. This overlay was conducted to elucidate the relationship between various land-use types and the occurrence of hot and cold spots in Kanchanaburi Province.

3. RESULTS AND DISCUSSION

3.1 Study of annual cumulative hotspot changes from 2012 to 2021

3.1.1 Study of annual cumulative hotspot occurrence frequency from 2012 to 2021

The analysis of annual cumulative hotspot occurrence frequencies from 2012 to 2021, employing the Suomi NPP satellite's VIIRS system, unveiled a varying pattern of changes. However, a distinct overall increase is evident in the cumulative hotspot count. In 2012, there were 4,190 hotspot locations, and in 2013, it slightly increased by 15.8% to 4,855 locations. In 2014, the cumulative hotspots surged to 8,680 locations, a significant increase of 78.9%. In 2015, the hotspots decreased to 5,235 locations, a decline of 39.7%. Subsequently, in 2020, the hotspot count rose to 13,293 locations, marking an increase of 34.7% from the previous year. In 2021, the cumulative hotspots decreased to 5,671 locations, reflecting a decline of 57.3% compared to 2020 in Figure 3.

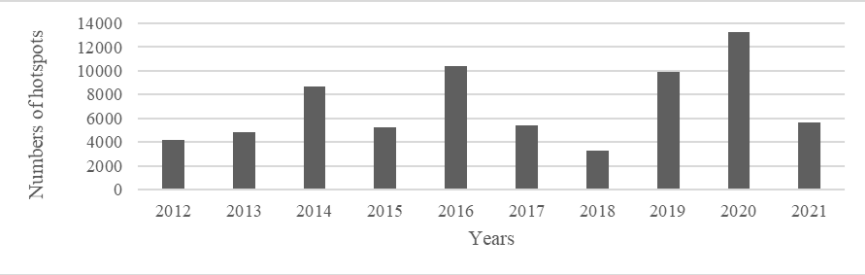

Figure 3. Annual cumulative hotspot occurrence and frequency changes from 2012 to 2021

While the occurrence pattern of cumulative hotspots in Kanchanaburi province demonstrates variability, a noticeable upward trajectory is evident in the cumulative hotspot count when assessing the frequency of cumulative hotspot occurrences from 2012 to 2021.

3.1.2 Monthly cumulative hotspot occurrence frequency from January to December 2012 - 2021

For the investigation of monthly cumulative hotspot occurrence frequency, data from the Suomi National Polar-orbiting Partnership (S-NPP) satellite's VIIRS system were utilized. The hotspot occurrence data were categorized on a monthly basis, spanning January to December, covering years 2012 to 2021 (see Figure 4).

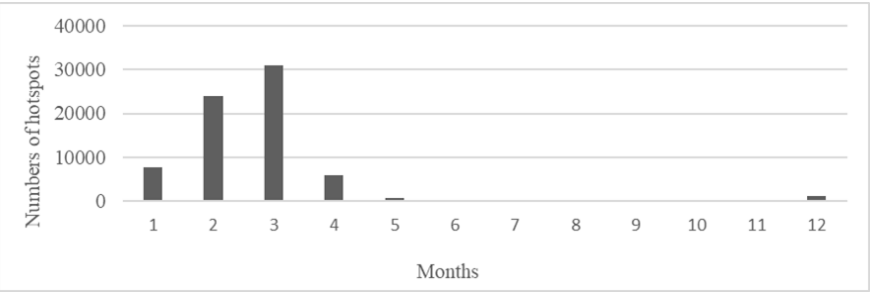

Figure 4. Monthly cumulative hotspot occurrence frequency from January to December 2012 to 2021.

It is evident that there is an increasing accumulation of hotspot from January-May, and December of each year. The buildup of hotspot begins gradually from mid-December and continues to increase until March. Subsequently, the cumulative hotspot decreases from April until mid-May of each year. This pattern is attributed to the dry season and the agricultural harvest period in Kanchanaburi province.

3.1.3 Monthly Fire Radiative Power (FRP) of cumulative hotspots

For the investigation of monthly Fire Radiative Power (FRP) of cumulative hotspots, the data on hotspot occurrences from the Suomi NPP satellite's VIIRS system for each year were categorized into monthly intervals from January to December. Subsequently, the total Fire Radiative Power of cumulative hotspots was computed on a monthly basis for the years 2012 to 2021. The findings reveal that the pattern of Fire Radiative Power distribution follows a similar trend to the monthly accumulation of hotspot occurrences (see Figure 5).

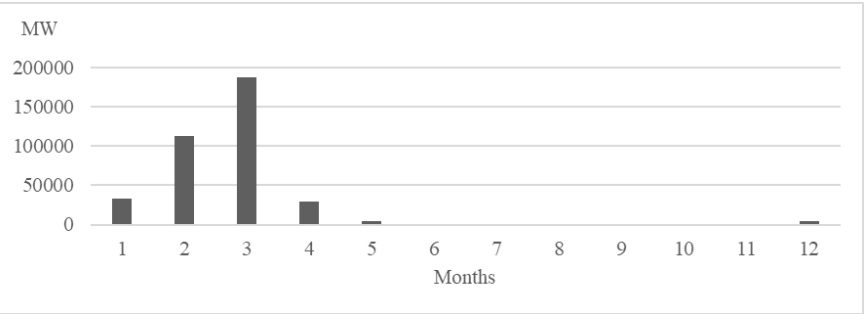

Figure 5. Monthly Fire Radiative Power (MW) of cumulative hotspots from 2012 to 2021.

The Fire Radiative Power of cumulative hotspots begins in December and undergoes a notable increase in January and February. The peak Fire Radiative Power is observed in March, succeeded by a gradual decline in April and May. The preponderance of cumulative hotspots falls into the 'VERY LOW: VL' category, followed by 'LOW: L,' 'MODERATE: M,' and 'HIGH: H,' as illustrated in Figure 6. Furthermore, the occurrence of cumulative hotspots during different time intervals Morning (4:00-8:00), Day (8:00-17:59), and Night (18:00-24:00) revealed that the majority of hotspots took place during the Morning, followed by Night, with the fewest occurrences observed during the Day, as delineated in Table 2.

Figure 6. Percentage of cumulative hotspot occurrence in relation to Fire Radiative Power.

Table 2. Fire Radiative Power of cumulative hotspots over time intervals.

Time	H	M	L	VL	Grand Total
Morning (4.00-8.00)	147	437	3048	38701	42333
Day (8.00-17.59)	0	0	0	79	79
Night (18.00-24.00)	0	8	35	28413	28456
Grand Total	**147**	**445**	**3083**	**67193**	**70868**

3.1.4 Spatial Analysis of cumulative hotspots for the years 2012-2021

For the spatial analysis of the hotspots for the years 2012-2021 using spatial autocorrelation through Getis-Ord statistics, the Incremental Spatial Autocorrelation analysis results were employed to determine the appropriate distance for the analysis.

The Incremental Spatial Autocorrelation analysis is a spatial autocorrelation analysis that tests the range of distances against the intensity of spatial clustering. The analysis utilizes the z-score, and by graphing the z-score values against the distance or Band Width, the Band Width value at the first peak or highest point of the graph indicates the level of spatial clustering. It was found that the Band Width ranges from 5,400 to 8,800 meters, with an average value of 7,190 meters, as shown in Table 3.

Table 3. Band Width results from Incremental Spatial Autocorrelation analysis.

Years	Band Width (meters)
2012	7000
2013	7900
2014	7700
2015	7300
2016	8800
2017	5400
2018	7200
2019	7400
2020	5600
2021	7600

The results of the spatial analysis of the hotspots for the years 2012-2021 using spatial autocorrelation through Getis-Ord statistics revealed that forested areas and agricultural areas, particularly field crops in the Sangkhla Buri, Thong Pha Phum, and Si Sawat districts, exhibit hotspots each year (see Figure 7).

By employing the results of the spatial analysis through Getis-Ord statistics to create a correlation table to study the Fire Radiative Power (FRP) characteristics and the occurrence of cumulative hotspots, the table reveals that 85% of hotspots in Kanchanaburi province from 2012-2021 demonstrate a spatial randomness pattern, as show in Table 4.

Table 4. The characteristics of fire intensity clusters.

Class	Number of Fire Counts	Percentage %	Average of FRP	Fire Intensity Class
Cold spot (99% CI)	420	1	3.254	VL
Cold spot (95% CI)	1561	2	3.307	VL
Cold spot (90% CI)	1738	2	3.038	VL
Not significant	60214	85	4.543	VL
Hot spot (90% CI)	777	1	7.318	VL
Hot spot (95% CI)	1194	2	9.000	VL
Hot spot (95% CI)	4964	7	14.236	VL
Total	**70868**	**100**	**5.256**	

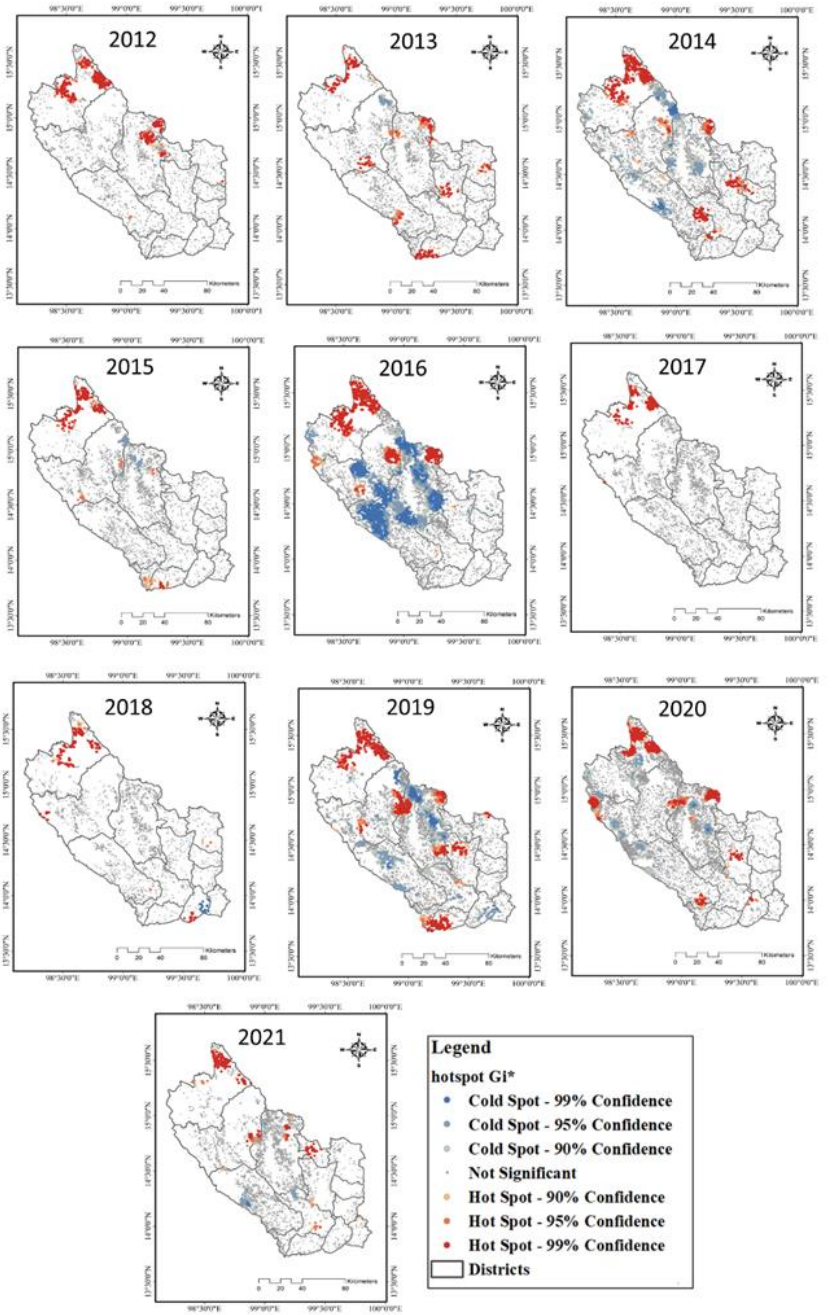

Figure 7. Hotspots for years 2012-2021 using spatial autocorrelation through Getis-Ord statistics.

From descriptive statistical data, it is evident that there is a difference in the average Fire Radiative Power (FRP) between hotspots and cold spots (see Figure 8). The average

FRP of hotspots is higher than that of cold spots, and the proportion of hotspot occurrence is greater than cold spot occurrences. The average FRP and the spatial pattern that occurs is statistically significant. Moreover, the majority of cumulative hotspot types are categorized as "Very Low".

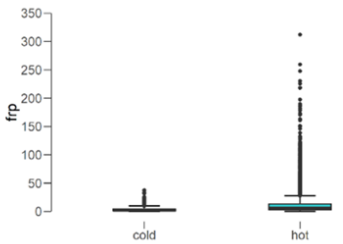

	FRP	
	Cold spots	Hotspots
Count	3719	6935
Missing	0	0
Mean	3.175	12.560
Std. Deviation	3.319	20.084
Minimum	0.110	0.180
Maximum	37.440	312.230

Figure 8. Descriptive statistical data for Fire Radiative Power (FRP) of hotspots and cold spots.

3.2 Study of the relationship between geographic factors and spatial patterns of cumulative hotspots

The analysis reveals that FRP has a negative correlation with slope and a positive correlation with elevation. This aligns with Figure 6, where hotspots tend to recur annually, primarily in areas with high elevation and predominantly hilly terrain including Sangkhla Buri, Thong Pha Phum, and Si Sawat districts. The aspect has no statistical significance. The statistical analysis using T-Test indicates that FRP values increase significantly when the elevation is higher in both hotspots and cold spots (see Table 5).

Table 5. The Pearson correlation coefficients.

	FRP and Slope(°)	FRP and Elevation(m)	FRP and Aspect(°)
Pearson's r	-0.080	0.024	0.030
p-value	< .001*	< .001*	0.363

3.3 Study of the relationship between land use and spatial patterns of cumulative hotspots

The investigation into the relationship between land use and the spatial patterns of cumulative hotspots involves overlaying the spatial pattern of hotspots with land use data and then explaining it in terms of the percentage of hotspots and cold spots within the cumulative hotspot areas in Kanchanaburi province. Subsequently, this information is presented in the form of a table depicting the correlation between land use and hotspots as well as cold spots (Table 6).

According to Table 6, 84.7% of hotspots and 92% of cold spots occur within forested areas, including non-deciduous forests, deciduous forests, and cultivated forests. The subsequent tier consists of agricultural lands, including field crops and rice fields, perennial plantations, fruit orchards and grass fields and facilities for animal husbandry. Hotspots account for 13.1% while cold spots make up 7.4% of this land type.

Table 6. Correlation between Land Use and Hotspots/Cold spots

Land Cover	Cold Spots	%	Hot Spots	%
agricultural	275	7.4	910	13.1
forests	3422	92.0	5871	84.7
Miscellaneous	15	0.4	129	1.9
Urban	7	0.2	25	0.3
Grand Total	**3719**	100	6935	100

4. DISCUSSION

Based on the tracking of changes in cumulative hotspot occurrences from 2012-2021, it is evident that hotspots are distributed throughout all districts of Kanchanaburi province. High levels of cumulative hotspots are observed during the period from December to May of each year. Districts with the highest hotspot occurrences are Si Sawat, followed by Thong Pha Phum, Sai Yok, Sangkhla Buri, Mueang Kanchanaburi, Bo Phloi, Lao Khwan, Nong Prue, Dan Makham Tia, Tha Muang, Huay Kra Jao, Phanom Thuan and Tha Maka districts. This seasonal hotspot distribution aligns with the dry season, while the reduced hotspot occurrences correspond to the rainy season. This relationship is influenced by various climatic factors, such as the number of rainy days, atmospheric pressure, relative humidity, and temperature (Hysa et al., 2021; Melo, et al., 2024; Yue, et al., 2023). Additionally, the rainy season is a period of vigorous plant growth followed by an abundance of fuel for wildfires during the subsequent dry season. Furthermore, hotspot occurrences are found to share similar spatial and environmental factors (Cizungu et al., 2021; Shekede et al., 2021). Areas with higher elevations exhibit a positive correlation with FRP, indicating that mountainous regions tend to have higher hotspot occurrences (Zúñiga-Vásquez & Pompa-García, 2019). This is evident in districts like Si Sawat, Thong Pha Phum, Sai Yok, and Sangkhla Buri.

FRP data from the VIIRS Suomi NPP system provide insights into the thermal energy released from fuel combustion (Kganyago & Shikwambana, 2019). In the case of cumulative hotspot spatial patterns within Kanchanaburi province, the majority fall into the category of "no significance," accounting for 85%. Hotspots comprise 10%, while cold spots make up 5%. The majority of cumulative hotspots remain as areas of very low thermal energy, occurring predominantly in dense forests and due to agricultural activities (Cizungu et al., 2021).

For the study of the relationship between land use and the spatial pattern of cumulative hotspots, it is evident that hotspot and cold spot occurrences align with the geographical characteristics of Kanchanaburi province. The northern and western regions are characterized by forests and mountains, while the northeastern and some northern parts consist of dry expansive plains alternating with gentle hills, consisting of mixed forests, savanna forests, and dry evergreen forests. However, due to the rain shadow effect, these areas receive minimal rainfall. The areas among the top three districts with the highest cumulative hotspots are Si Sawat, Thong Pha Phum, and Sai Yok, which boast seven national parks, including Thong Pha Phum National Park, Lam Khlong Ngu National Park, Khao Laem National Park, Erawan National Park, Sri Nakarin Dam National Park, Chaloem Rattanakosin National Park and Sai Yok National Park. As a result, forested lands dominate the majority of land use, and hotspots and cold spots are identified within tree cover, grassland, and cropland areas, respectively, indicating the outcomes of human activities such as forest product collection, illicit farming, and livestock in forested areas (Adámek et al., 2018; Phonphan, 2020).

The Gi* statistical analysis reveals the spatial pattern of cumulative hotspots and the hotspot and cold spot occurrence in forested and agricultural areas. Additionally, utilizing data from the VIIRS Suomi NPP system provides information on burned areas with a resolution of 375x375 meters, surpassing the resolution of MODIS, which is 1,000 x 1,000 meters (Marsha & Larkin, 2022). This helps ascertain the recurrence of hotspots and cold spots within Kanchanaburi province. In relation to vegetation types and land use, the forest areas are thick forests that encompass deciduous forests, non-deciduous forests, and cultivated forests, while agricultural lands include field crops, garden plants and rice fields, perennial plantations, fruit orchards, and grass fields and

facilities for animal husbandry. Lastly, miscellaneous or vacant lands consist of grasslands and shrubs.

For future studies, especially to comprehend the impacts of climate change on cumulative hotspot occurrences, it is advisable to incorporate climate data, such as precipitation volume, number of rainy days, average temperature, relative humidity, and atmospheric pressure, to analyze more complex relationships. This will aid in understanding and addressing the issues stemming from rising global temperatures (Brotons et al., 2013).

5. CONCLUSION

This research article focused on cumulative hotspots and their relationships with topographical factors and land use in Kanchanaburi province, Thailand. We employed data from the VIIRS system aboard the Suomi NPP satellite to analyze spatial autocorrelation. This methodology can be applied to various regions with similar spatial and environmental factors. However, this phenomenon is complex, and the occurrence of hotspot accumulation may vary based on different environmental conditions and factors. Besides natural factors, human-induced factors also play a significant role in many areas, as activities such as land clearing for agriculture or controlled burns to promote animal fodder can lead to the ignition of fires. The study reveals that both hotspot and cold spot occurrences in Kanchanaburi province take place within forested and agricultural areas. Hotspots are predominantly situated in mountainous regions. The outcomes of this research can assist relevant organizations, whether at the national level, such as the Ministry of Natural Resources and Environment, or at the local level, including provincial and sub-district administrative bodies or agencies working in the area to conduct resource management planning for prevention and suppression of forest fires. It can also assist post-fire recovery efforts contributing to addressing natural resource issues arising from the occurrence of cumulative hotspots and pollution resulting from hotspot burnings, especially within national park areas adjacent to villages or communities. This information is crucial in raising community awareness about the issue and helping monitor hotspot burning problems in neighboring community areas.

Author Contributions: Conceptualization, P.S. and C.L.; Validation, P.S.; Formal analysis, P.S.; Supervision, C.L. and A.S. All authors have read and agreed to the published version of the manuscript.

Competing Interests: The authors declare no conflict of interest.

Acknowledgments: This research received no external funding.

REFERENCES

Adámek, M., Jankovská, Z., Hadincová, V., Kula, E., & Wild, J. (2018). Drivers of forest fire occurrence in the cultural landscape of Central Europe. *Landscape Ecology, 33*(11), 2031-2045. https://doi.org/10.1007/s10980-018-0712-2

Akyürek, Ö. (2023). Spatial and temporal analysis of vegetation fires in Europe. *Natural Hazards, 117*(1), 1105-1124. https://doi.org/10.1007/s11069-023-05896-0

Anselin, L. (1995). Local indicators of spatial association—LISA. *Geographical Analysis, 27*(2), 93-115. https://doi.org/10.1111/j.1538-4632.1995.tb00338.x

Benesty, J., Chen, J., Huang, Y., Cohen, I. (2009). Pearson Correlation Coefficient. In Benesty, J., Chen, J., Huang, Y., & Cohen, I. (Eds.), *Noise reduction in speech*

processing (Vol. 2) (pp. 1-4). Springer Science & Business Media. https://doi.org/10.1007/978-3-642-00296-0_5

Brotons, L., Aquilué, N., De Cáceres, M., Fortin, M.-J., & Fall, A. (2013). How fire history, fire suppression practices and climate change affect wildfire regimes in Mediterranean landscapes. *PloS one, 8*(5), e62392. https://doi.org/10.1371/journal.pone.0062392

Cizungu, N. C., Tshibasu, E., Lutete, E., Mushagalusa, C. A., Mugumaarhahama, Y., Ganza, D., ... & Bogaert, J. (2021). Fire risk assessment, spatiotemporal clustering and hotspot analysis in the Luki biosphere reserve region, western DR Congo. *Trees, Forests and People, 5,* 100104. https://doi.org/10.1016/j.tfp. 2021.100104

de México, C. E. (2017). Spatial modeling of forest fires in Mexico: an integration of two data sources. *Bosque, 38*(3), 563-574.

Department of Pollution Control. (2020). *The 5-Year Strategic Plan (B.E. 2566 - 2570) of the Department of Pollution Control*. Retrieved 09/10/2023 from https://www.pcd.go.th/strategy/แผนปฏิบัติราชการระยะ-5-ปี-พ-ศ-2566-2570-ของกรมควบคุมมลพิษ

FIRMS. (2020). *Country Yearly Summary*. FIRM. Retrieved 25/03/2022 from https://firms.modaps.eosdis.nasa.gov/country/

Fu, Y., Gao, H., Liao, H., & Tian, X. (2021). Spatiotemporal Variations and Uncertainty in Crop Residue Burning Emissions over North China Plain: Implication for Atmospheric CO2 Simulation. *Remote Sensing, 13*(19), 3880. https://www.mdpi.com/2072-4292/13/19/3880

Fu, Y., Gao, H., Liao, H., & Tian, X. (2021). Spatiotemporal variations and uncertainty in crop residue burning emissions over North China plain: Implication for atmospheric co2 simulation. *Remote Sensing, 13*(19), 3880. https://doi.org/10.3390/rs13193880

Geo-Informatics and Space Technology Development Agency (Public Organization). (2020*). Report on the situation of forest fires and haze from satellite data for the year 2020*. Geo-Informatics and Space Technology Development Agency Retrieved 25/03/2022 from https://fire.gistda.or.th/fire_report/Fire_2563.pdf

Getis, A., & Ord, J. K. (1992). The Analysis of Spatial Association by Use of Distance Statistics. *Geographical Analysis, 24*(3), 189-206. https://doi.org/10.1111/j.1538-4632.1992.tb00261.x

Hazaymeh, K., Almagbile, A., & Alomari, A. H. (2022). Spatiotemporal Analysis of Traffic Accidents Hotspots Based on Geospatial Techniques. *ISPRS International Journal of Geo-Information, 11*(4), 260. https://doi.org/10.3390/ijgi11040260

Hysa, A., Spalevic, V., Dudic, B., Roșca, S., Kuriqi, A., Bilașco, Ș., & Sestras, P. (2021). Utilizing the available open-source remotely sensed data in assessing the wildfire ignition and spread capacities of vegetated surfaces in Romania. *Remote Sensing*, 13(14), 2737. https://doi.org/10.3390/rs13142737

Kanchanaburi Provincial Statistical Office. (2022). *Kanchanaburi Province Statistical Report 2022.* Kanchanaburi Provincial Statistical Office http://kanchanaburi.nso.go.th/index.php?option=com_content&view=article&id=957:2565&catid=120:2021-01-15-22-48-53&Itemid=579

Kganyago, M., & Shikwambana, L. (2019). Assessing Spatio-Temporal Variability of Wildfires and their Impact on Sub-Saharan Ecosystems and Air Quality Using Multisource Remotely Sensed Data and Trend Analysis. *Sustainability, 11*(23), 6811. https://doi.org/10.3390/su11236811

Kumharn, W., Sudhibrabha, S., Hanprasert, K., Janjai, S., Masiri, I., Buntoung, S., ... & Jankondee, Y. (2024). Estimating hourly full-coverage PM2. 5 concentrations

model based on MODIS data over the northeast of Thailand. *Modeling Earth Systems and Environment, 10*(1), 1273-1280. https://doi.org/10.1007/s40808-023-01839-7

Land Development Department. (2023). *Land Use.* Land Development Department. Retrieved 20/01/2023 from: http://webapp.ldd.go.th/Soilservice/

Lanorte, A., Danese, M., Lasaponara, R., & Murgante, B. (2013). Multiscale mapping of burn area and severity using multisensor satellite data and spatial autocorrelation analysis. *International Journal of Applied Earth Observation and Geoinformation, 20*, 42-51. https://doi.org/10.1016/j.jag.2011.09.005

Li, R., He, X., Wang, H., Wang, Y., Zhang, M., Mei, X., ... & Chen, L. (2022). Estimating emissions from crop residue open burning in Central China from 2012 to 2020 using statistical models combined with satellite observations. *Remote Sensing, 14*(15), 3682. https://doi.org/10.3390/rs14153682

Marsha, A. L., & Larkin, N. K. (2022). Evaluating satellite fire detection products and an ensemble approach for estimating burned area in the United States. *Fire, 5*(5), 147. https://doi.org/10.3390/fire5050147

Melo, K. D. S., Delgado, R. C., Pereira, M. G., & Ortega, G. P. (2024). The Consequences of Climate Change in the Brazilian Western Amazon: A New Proposal for a Fire Risk Model in Rio Branco, Acre. *Forests*, 15(1), 211. https://doi.org/10.3390/f15010211

Mesquitela, J., Elvas, L. B., Ferreira, J. C., & Nunes, L. (2022). Data Analytics Process over Road Accidents Data—A Case Study of Lisbon City. *ISPRS International Journal of Geo-Information, 11*(2), 143. https://doi.org/10.3390/ijgi11020143

Mpakairi, K. S., Tagwireyi, P., Ndaimani, H., & Madiri, H. T. (2019). Distribution of wildland fires and possible hotspots for the Zimbabwean component of Kavango-Zambezi Transfrontier Conservation Area. *South African Geographical Journal, 101*(1), 110-120. https://doi.org/10.1080/03736245.2018.1541023

Mupfiga, U. N., Mutanga, O., Dube, T., & Kowe, P. (2022). Spatial Clustering of Vegetation Fire Intensity Using MODIS Satellite Data. *Atmosphere, 13*(12), 1972. https://doi.org/10.3390/atmos13121972

NASA JPL (2020). *NASADEM Merged DEM Global 1 arc second V001 [Data set]. NASA EOSDIS Land Processes DAAC.* NASA JPL Accessed 2020-12-30 from https://10.5067/MEaSUREs/NASADEM/NASADEM_HGT.001

Phonphan, W. (2020). Analysis Forest Fire Cause and Different Land Use Within Buffer Zones in Kanchanaburi Province, Thailand. In Monprapussorn, S., Lin, Z., Sitthi, A., & Wetchayont, P. (Eds.), *Geoinformatics for Sustainable Development in Asian Cities* (pp. 118-127). Springer International Publishing.

Reddy, C. S., Unnikrishnan, A., Bird, N. G., Faseela, V. S., Asra, M., Manikandan, T. M., & Rao, P. V. N. (2020). Characterizing vegetation fire dynamics in Myanmar and South Asian Countries. *Journal of the Indian Society of Remote Sensing, 48,* 1829-1843. https://doi.org/10.1007/s12524-020-01205-5

Royal Thai Survey Department. (2023). Thailand - Subnational Administrative Boundaries. Royal Thai Survey Department. Retrieved 20/01/2023 from https://data.humdata.org/dataset/cod-ab-tha

Schroeder, W., Oliva, P., Giglio, L., & Csiszar, I. A. (2014). The New VIIRS 375 m active fire detection data product: Algorithm description and initial assessment. *Remote Sensing of Environment*, 143, 85-96. https://doi.org/10.1016/j.rse. 2013.12.008

Shekede, M. D., Gwitira, I., & Mamvura, C. (2021, 2021/05/09). Spatial modelling of wildfire hotspots and their key drivers across districts of Zimbabwe, Southern

Africa. *Geocarto International, 36*(8), 874-887. https://doi.org/10.1080/10106049.2019.1629642

Tzoumas, G., Pitonakova, L., Salinas, L., Scales, C., Richardson, T., & Hauert, S. (2023). Wildfire detection in large-scale environments using force-based control for swarms of UAVs. *Swarm Intelligence, 17*(1-2), 89-115. https://doi.org/10.1007/s11721-022-00218-9

Unnikrishnan, A., & Reddy, C. S. (2020). Characterizing distribution of forest fires in Myanmar using earth observations and spatial statistics tool. *Journal of the Indian Society of Remote Sensing, 48*, 227-234. https://doi.org/10.1007/ s12524-019-01072-9

Vadrevu, K. P., Lasko, K., Giglio, L., Schroeder, W., Biswas, S., & Justice, C. (2019). Trends in vegetation fires in south and southeast Asian countries. *Scientific reports, 9*(1), 1-13. https://doi.org/10.1038/s41598-019-43940-x

Vadrevu, K., Eaturu, A., Casadaban, E., Lasko, K., Schroeder, W., Biswas, S., ... & Justice, C. (2022). Spatial variations in vegetation fires and emissions in South and Southeast Asia during COVID-19 and pre-pandemic. *Scientific Reports*, 12(1), 18233. https://doi.org/10.1038/s41598-022-22834-5

Wongnakae, P., Chitchum, P., Sripramong, R., & Phosri, A. (2023). Application of satellite remote sensing data and random forest approach to estimate ground-level PM2. 5 concentration in Northern region of Thailand. *Environmental Science and Pollution Research*, 30(38), 88905-88917. https://doi.org/10.1007/s11356-023-28698-0

Ye, J., Wu, M., Deng, Z., Xu, S., Zhou, R., & Clarke, K. C. (2017). Modeling the spatial patterns of human wildfire ignition in Yunnan province, China. *Applied Geography, 89*, 150-162. https://doi.org/10.1016/j.apgeog.2017.09.012

Yu, J., Jiang, X., Zeng, Z. C., & Yung, Y. L. (2024). Fire Monitoring and Detection Using Brightness-Temperature Difference and Water Vapor Emission from the Atmospheric InfraRed Sounder. *Journal of Quantitative Spectroscopy and Radiative Transfer,* 108930. https://doi.org/10.1016/j.jqsrt.2024.108930

Yue, W., Ren, C., Liang, Y., Lin, X., Yin, A., & Liang, J. (2023). Wildfire Risk Assessment Considering Seasonal Differences: A Case Study of Nanning, China. *Forests*, 14(8), 1616. https://doi.org/10.3390/f14081616

Zhang, T., de Jong, M. C., Wooster, M. J., Xu, W., & Wang, L. (2020). Trends in eastern China agricultural fire emissions derived from a combination of geostationary (Himawari) and polar (VIIRS) orbiter fire radiative power products. *Atmos. Chem. Phys., 20*(17), 10687-10705. https://doi.org/10.5194/acp-20-10687-2020

Zúñiga-Vásquez, J. M., & Pompa-García, M. (2019). The occurrence of forest fires in Mexico presents an altitudinal tendency: a geospatial analysis. *Natural Hazards, 96*(1), 213-224. https://doi.org/10.1007/s11069-018-3537-z